

Mapping Pre-Fire Forest Conditions with NOAA-AVHRR Images in the Northwest Territories, Canada

Steven Oldford, Brigitte Leblon (*) and Lisa Gallant

Organization: Faculty of Forestry, University of New Brunswick, Fredericton, NB, Canada

Phone: (506) 453-4924

Email: bleblon@unb.ca

M.E. Alexander

Organization: Canadian Forest Service, Edmonton, Canada

Phone: (780) 435-7346

Email: malexand@nrcan.gc.ca

(*) Corresponding author

ABSTRACT

In Canada, fire danger maps are generated daily by the Canadian Forest Fire Danger Rating System from weather station records. Such maps are limited spatially because they are produced from point-source weather measurements. Thus, remote sensing was investigated as an alternative. Thermal infrared NOAA-AVHRR images were used to describe pre-fire conditions of 24 large fires, occurring in 1994 in the Northwest Territories, Canada. Values of daily mean surface temperatures and fire weather index for burned areas were compared with those of surrounding unburned areas during an 11 day period prior to and on the day of fire ignition. It was hypothesized that: (i) mean surface temperature will increase as fire ignition dates approach; (ii) mean surface temperature within burned areas will be greater than within unburned areas; (iii) surface temperature will be positively related to the fire weather index. A positive trend in mean surface temperature was observed as ignition dates approached, but high percentages of cloud contamination made it difficult to follow each fire day to day. Similar trends were observed over unburned areas. A good relationship was found between surface temperatures and fire weather indices. Limitations and possible improvements of this study are also presented.

Keywords: NOAA-AVHRR surface temperature, fire weather index, fire danger, Northwest Territories, northern boreal forests

1. Introduction

Covering approximately 42% of its land surface, forests are an important natural resource in Canada (Canadian Council of Forest Ministers, 2001). Canada's boreal forest accounts for 77% of this area (Rowe, 1972). Fire is a natural and necessary component within the boreal forest and most of Canada's forest fires occur within its limits (Van Wagner, 1990). However, forest fires are very costly as attempts are made to protect lives, property and forest resources (Stocks et al., 1989). In 1999, 1.2 million ha burned in Canada despite the spending of \$270 million on forest fire protection (Canadian Council of Forest Ministers, 2001).

In Canada, daily fire danger and behavior are predicted by the Canadian Forest Fire Danger Rating System (CFFDRS). This semi-empirical modular system utilizes weather, fuel, topography and ignition parameters as inputs to rate fire danger through four subsystems (Stocks et al., 1989). One of these subsystems, the Fire Weather Index (FWI) system, represents a relative measure of potential mid-afternoon fire danger (Canadian Forestry Service, 1987). Inputs to the system are measured daily at 12:00 LST from weather station dry bulb temperature, relative humidity, 10m high open wind speed and 24hour precipitation measurements (Stocks et al., 1989). The FWI system comprises three moisture codes, two intermediate indices and the FWI itself. The three moisture codes represent moisture contents of surface litter fine fuels (FFMC) with a time lag of two-thirds of a day; moderate depth loosely compact duff (DMC) with a time lag of 12 days; and deep layer compact organic matter (DC) with a time lag of 52 days. The two intermediate indices, derived from the three moisture codes and wind speeds, provide a measure of the rate of initial fire spread (ISI), and the total fuel available for combustion (BUI). The FWI itself is obtained from the combination of both intermediate indices (Canadian Forestry Service, 1987).

The FWI system is limited because it only produces estimates of fire danger for large geographic regions and does not consider environmental conditions at finer spatial scales. This is because it does not consider different forest types, topographic effects and is based on weather station readings, which are often widely dispersed with poor spatial resolution (Flannigan and Wotton, 1989; Stocks et al., 1989).

Due to these limitations, satellite remote sensing is a promising alternative. Satellite remote sensing can cover large spatial regions; avoid resource destruction; gather data from less accessible areas; and retrieve this information on a regular basis (Leblon, 2001). Several CFFDRS parameters can be mapped using satellite remote sensing. They are related not only to topography, plant phenology and fuel types, but also to fuel moisture conditions. Fuel type can be mapped from high spatial resolution optical or radar images as in classical vegetation mapping (Leblon et al., 2001). In previous studies reviewed by Leblon (2001), fuel moisture has been estimated primarily from NOAA-AVHRR normalized difference vegetation index (NDVI) images (e.g., Paltridge and Barber, 1988; Illera et al., 1996; Burgan et al., 1998). Thermal infrared NOAA-AVHRR images were also used (e.g., Dominguez et al., 1994; Chuvieco et al., 1999; Strickland et al., 2001) because surface temperatures (T_s) increase with droughtiness levels (Pierce et al., 1990). Most of these studies strictly considered fire danger parameters, without considering actual fire occurrences. Vidal et al. (1994) and Prosper-Laget et al. (1995) showed, that in the case of Mediterranean forests, the number of fires was related to spectral indices computed from NOAA-AVHRR T_s images. Strickland et al. (2001) applied the method of Vidal et al. (1994) over northern boreal forests to describe fire danger parameters from thermal infrared NOAA-AVHRR images. Desbois and Vidal (1995) showed that over Mediterranean forests, fire ignition primarily occurred in the hot zones of NOAA-AVHRR T_s images acquired just before fire ignition date. Similarly, following Desbois and Vidal (1995), this study investigated the use of these images for describing actual pre-fire conditions over northern boreal forests. The study had three hypotheses. First, as forest fire ignition dates approach, mean T_s within burned areas will increase in parallel to increasing water stress, which renders their vegetation more susceptible to fire. Second, prior to fire ignitions, mean T_s within burned areas will be greater than unburned areas because unburned vegetation will have a lower degree of water stress. Third, prior to fire ignition, T_s will be positively related to the FWI because both increase with decreasing fuel moisture. To test these hypotheses, NOAA 11-AVHRR images were used to map pre-fire T_s and FWI values in the regions of 24 large forest fires of more than 2000ha occurring during the 1994 fire season in the Northwest Territories, Canada.

2. Material and Methods

The study area for this research was located in the MacKenzie River basin, Northwest Territories, Canada, between 57°36'Lat.N. and 71°27'Lat.N. and between 110°39'Long.W. and 138°18'Long.W. It fell within the Taiga Plains Ecozone of Canada, and included transitional, boreal (taiga), mixed and deciduous forest zones. Forests located in this region experienced a high fire occurrence between 1980 and 1989 and in 1994 (Gallant, 1998). It was predicted that beyond the year 2010, the annual area burned within the basin would increase to 160% of its 1980 level by the years 2050 (Rothman and Herbert, 1997).

This study used cartographic, weather data and satellite imagery acquired at various spatial scales during the 1994 fire season over the MacKenzie River basin (Table 1).

Table 1 Materials used in this study

Data Type	Variable	Spatial Resolution	Source
Spectral	NDVI images	Pixel of 1km ²	NOAA 11-AVHRR study area images (Gallant, 1998)
	T_s images	Pixel of 1km ²	NOAA 11-AVHRR study areas images (Gallant, 1998)
Weather	Daily FWI Maps	IDW point interpolation	Yukon and Northwest Territories weather stations (Canadian Forestry Service)
Cartographic	Forest Fires Maps	<various>	1994 Northwest Territories Forest Fire Coverage (NWT Government)
	Elevation Maps	Pixel of 1km ²	Digital Elevation Map of Canada (Geogratis Canada)

Spectral data, utilized in mapping T_s and NDVI were extracted from NOAA 11-AVHRR images obtained during an 11 day period prior to and on the day of fire ignition. These images were acquired between 22 and 24 UT, which corresponds to the afternoon locally. Each image belonged to the GEOCOMP database (Robertson et al., 1992) and thus was georeferenced according to a Lambert conformal conic projection. Each image had a spatial resolution of 1km² and was constituted of eight bands: two optical bands in the red and near-infrared; three thermal infrared bands; and three bands used to give each pixel a sun zenith angle, a view zenith angle and a relative sun-sensor azimuth angle. T_s and NDVI images were processed using PCI's EASI/PACE software following the methods detailed in Gallant (1998). T_s images were used to assess fire danger and NDVI images were used to assess cover types within the study area.

Twenty-four forest fires, which burned during the 1994 fire season in the study area, were extracted from the Northwest Territories forest fire map (Table 2). For each fire, a GIS polygon was used to delineate burned areas over corresponding images. Burned areas were defined by the number of NOAA 11-AVHRR land feature pixels contained within its forest fire map polygon. In addition to burned areas, adjacent unburned areas of each fire were delineated on the images. Unburned

areas consisted of land features within a zone twice the size of a rectangle, enclosing the burned area. For each fire zone, elevation maps extracted from the GEOGRATIS database were used to describe the topography (GEOGRATIS 2001). FWI data computed daily at 35 weather stations from the Northwest Territories and Yukon Territories were interpolated using an inverse distance weighted interpolation method to produce FWI maps. These maps were then converted into a PCI format to produce FWI images which were used to describe drought conditions and fire danger levels. All maps were produced using ESRI's ArcInfo and ArcView GIS software.

Table 2 Forest fire positions, start dates, number of burned pixels and number of unburned pixels for 24 large forest fires zones within the study area

Fire ID	Latitude	Longitude	Ignition Date		Number of Burned Area Pixels (km)	Number of Unburned Area Pixels (km)
			Date	Julian Date		
fs038	63°59'	126°13'	Jul 15, 94	196	60	299
fs061	63°53'	119°49'	Jul 16, 94	197	331	3225
fs063	63°49'	119°08'	Jul 16, 94	197	198	972
fs078	62°52'	120°21'	Jul 18, 94	199	5259	36166
fs088	61°36'	123°05'	Jul 30, 94	211	700	4573
fs091	60°33'	119°37'	Aug 3, 94	215	163	1137
fs092	63°48'	126°16'	Aug 4, 94	216	24	143
fs099	62°19'	123°33'	Aug 10, 94	222	39	174
fs102	63°48'	125°47'	Aug 15, 94	227	215	1225
fs103	63°06'	124°50'	Aug 9, 94	221	31	137
fs104	63°09'	125°29'	Aug 9, 94	221	159	933
fs105	63°56'	125°14'	Aug 23, 94	235	132	820
hy001	61°23'	117°08'	May 25, 94	145	149	884
hy038	61°48'	115°34'	Aug 5, 94	217	196	670
jf013	60°55'	123°47'	Jul 19, 94	200	117	701
vq033	64°17'	124°16'	Jul 16, 94	197	2061	25360
vq039	64°39'	121°50'	Jul 17, 94	198	188	1215
vq049	64°22'	120°43'	Jul 29, 94	210	131	666
vq057	64°38'	127°17'	Aug 4, 94	216	69	411
zf058	63°51'	118°00'	Jul 9, 94	190	511	2684
zf079	64°30'	118°32'	Jul 14, 94	195	397	1881
zf107	62°53'	117°50'	Jul 17, 94	198	174	809
zf125	63°27'	113°12'	Jul 19, 94	200	310	1288
zf149	62°37'	117°32'	Jul 26, 94	207	576	6955

FWI, T_s and NDVI images were extracted for each fire zone and corresponding pixel values were recorded from the burned and unburned areas during the 11 day period prior to and on the day of fire ignition. T_s and NDVI images were not considered if more than half of their pixels were contaminated by clouds, aerosols, snow or ice. Means, standard deviations and coefficient of variations of FWI, T_s and NDVI land features values were calculated for the 11 burned and unburned images of each fire zone using the SAS statistical software package.

3. Results and discussion

3.1 Seasonal Variations of T_s and NDVI

Mean T_s values of burned areas did not differ significantly from corresponding unburned areas. The range of variation was 17.17 to 37.47°C for burned areas and 16.02 to 36.61°C for the unburned areas (Table 3). In each case, the coefficient of variation associated with T_s was less than 11%, which meant that mean T_s was representative over the fire zones. Corresponding mean NDVI values were very similar between burned and unburned areas, ranging from 0.4 to 0.65, but in each case, NDVI values were more variable than T_s values. This meant that cover types were more variable over each fire zone. A low mean NDVI value was observed within the burned area of fire “zf149” on Julian date 207. This NDVI corresponded to the day of fire ignition and may be low because the area was already burning. This NDVI values also corresponded to the highest recorded mean T_s (37.48°C), probably because burning fires produce hot spots in T_s images.

Table 3 Mean T_s , NDVI and FWI values for clear burned and unburned area images during the 11 day period prior to and on the day of fire ignition (standard deviation and coefficient of variation calculated for T_s and NDVI)

Fire id	Day Before Fire	Julian Date	Burned Area							Unburned Area						
			T_s			NDVI			FWI	T_s			NDVI			FWI
			mean	std	cv	mean	std	cv	mean	mean	std	cv	mean	std	cv	mean
fs038	4	192	31.68	1.06	3.33	0.48	0.05	11.20	19.00	32.03	0.93	2.90	0.50	0.08	16.58	19.17
fs061	3	194	30.87	0.80	2.59	0.49	0.05	9.36	13.77	31.06	1.67	5.39	0.55	0.07	12.16	13.65
	2	195	32.79	0.93	2.85	0.50	0.05	9.60	14.78	32.56	1.88	5.78	0.55	0.07	11.99	14.72
	1	196	33.11	1.18	3.56	0.45	0.05	11.17	17.11							
fs063	3	194	29.98	1.20	4.01	0.49	0.05	9.36	13.37	31.63	1.49	4.72	0.55	0.07	12.16	13.37
	2	195	30.76	1.24	4.02	0.50	0.05	9.60	15.00	33.01	1.55	4.69	0.55	0.07	11.99	15.00
	1	196	32.46	1.47	4.52	0.45	0.05	11.17	18.00							
fs078	5	194	32.58	1.31	4.02	0.53	0.05	9.00	11.44	31.74	1.79	5.65	0.54	0.06	10.46	11.86
	4	195	33.08	1.94	5.86	0.50	0.06	12.03	10.71	32.50	2.03	6.25	0.52	0.05	10.36	11.31
	3	196	34.89	2.09	5.99	0.47	0.06	13.89	15.43							
fs088	10	201	27.04	1.61	5.97	0.64	0.07	11.05	31.11	26.81	1.84	6.85	0.67	0.10	14.29	30.89
	9	202	28.64	2.34	8.18	0.61	0.10	15.77	4.12	27.03	1.96	7.24	0.67	0.11	16.65	4.30
	6	205	37.17	1.45	3.90	0.50	0.06	11.71	19.18							
fs091	10	205	36.19	0.70	1.94	0.51	0.04	7.27	20.82	36.03	0.70	1.93	0.54	0.04	7.39	20.53
	9	206	36.80	0.50	1.36	0.49	0.02	4.79	27.40							
fs092	10	206	36.01	0.86	2.39	0.51	0.05	8.82	23.00	36.61	1.69	4.62	0.47	0.05	11.46	23.23
	9	207								33.36	1.46	4.37	0.43	0.04	9.88	17.43
fs105	0	235	18.81	2.03	10.77	0.44	0.15	34.18	6.96	16.55	1.55	9.34	0.60	0.08	13.63	6.61
hy001	6	139	17.17	1.17	6.84	0.38	0.07	18.53	6.00	16.02	1.15	7.16	0.45	0.06	13.27	5.89
hy038	7	210	32.22	0.81	2.51	0.46	0.05	11.25	25.17	32.02	0.64	2.01	0.47	0.04	9.42	25.26
	2	215	27.58	0.88	3.19	0.41	0.06	13.91	30.16							
jf013	6	194	25.80	2.27	8.81	0.53	0.08	15.03	11.00	27.89	2.83	10.13	0.59	0.10	16.76	11.00
	0	200	28.80	1.61	5.57	0.60	0.07	12.16	17.00							
vq033	4	193	31.55	1.70	5.38	0.53	0.05	12.10	17.03							
	3	194	34.40	1.86	5.42	0.56	0.06	10.98	17.36	33.42	2.33	6.99	0.48	0.06	11.05	17.47
	2	195	33.31	1.89	5.68	0.44	0.07	12.13	16.59	33.01	2.13	6.44	0.52	0.06	11.95	16.58
	1	196	35.01	1.89	5.40	0.43	0.06	13.00	16.77							
vq039	4	194	31.98	0.93	2.89	0.51	0.03	5.31	16.00							
	3	195	32.40	1.07	3.32	0.55	0.03	5.22	16.00	31.27	1.21	3.87	0.54	0.04	8.18	16.00
vq057	10	206	33.28	0.71	2.12	0.49	0.04	8.00	22.00	32.65	1.05	3.21	0.46	0.07	15.41	22.00
zf058	10	181	28.09	0.79	2.81	0.54	0.06	11.52	22.71	28.15	1.55	5.51	0.54	0.06	11.10	22.63
	6	185	31.73	0.95	2.98	0.48	0.06	13.40	25.00							
zf079	10	185	32.10	0.99	3.07	0.49	0.04	7.48	23.19							
	2	193	27.55	0.77	2.81	0.52	0.06	10.88	14.57							
	1	194	31.77	1.27	4.01	0.48	0.06	13.07	15.00							
	0	195	32.50	1.25	3.85	0.50	0.06	11.14	16.71	32.63	1.49	4.58	0.51	0.06	11.48	16.34
zf107	4	194	31.96	0.80	2.50	0.43	0.07	16.39	13.00	31.83	1.16	3.65	0.45	0.07	14.97	13.21
	2	196	34.70	1.00	2.89	0.44	0.08	17.48	19.90	34.76	1.32	3.80	0.46	0.07	15.02	19.56
zf125	6	194	30.71	0.97	3.15	0.47	0.05	10.94	17.00							
	5	195	33.44	1.14	3.42	0.47	0.05	10.17	20.00							
zf149	0	207	37.48	1.31	3.50	0.33	0.04	11.29	20.39							

The range of T_s variation was similar to those observed with NOAA-AVHRR over Quebec coniferous forests (Goita et al., 1997), France maritime pine forests (Duchemin et al., 1999) and Mediterranean forests (Desbois, 1994; Prosper-Laget et al., 1995), as well as with weather tower measurements over BOREAS sites (Prince et al., 1998). The range of NDVI variation was similar to those observed with NOAA-AVHRR over Eastern Canadian coniferous and mixed forests (Goward et al., 1985; Deblonde & Cihlar, 1993; Goita et al., 1997), Montana coniferous forests (Nemani & Running, 1989; Burgan & Hartford, 1993; Nemani et al., 1993; Burgan et al., 1996), France maritime pine forests (Duchemin et al., 1999) and Mediterranean forests (Prosper-Laget et al., 1995; Illera, et al., 1995; Schmidt & Gitelson, 2000), as well as with airborne data over Montana coniferous forests (Hardy & Burgan, 1999) and BOREAS sites (Huemmrich et al., 1999).

3.2 T_s Evolution as a Function of Days Before Fire Ignition

Fires “fs099”, “fs102”, “fs103” and “fs104” had no clear images during the 11 day analysis period. Of the remaining 20 fires there were 40 burned and 24 unburned areas with images that were clear of contamination. Because of the lack of available clear images over each fire zone, it was impossible to conduct the analysis on an individual fire basis. Fires were pooled together and general trends were derived. In order see if T_s within burned areas would increase in parallel to increasing water stress, which rendered their vegetation more susceptible to fire, mean T_s values were graphed as a function of their acquisition date prior to fire ignition for burned areas (Figure 1) and unburned areas (Figure 2).

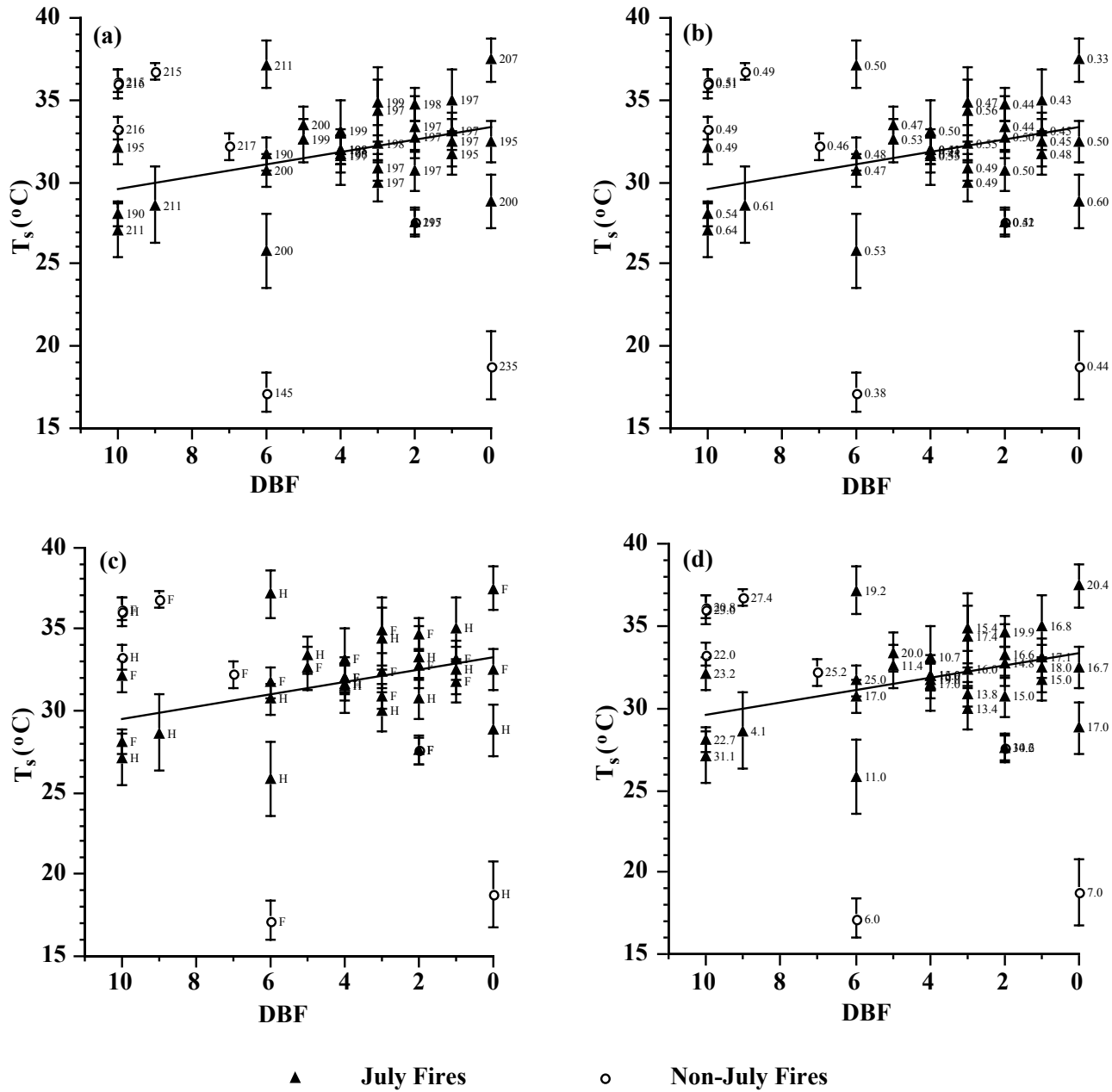


Figure 1 Scatter plots of mean T_s within burned areas versus days before fire ignition, for fires starting and not starting in July, labeled with (a) Julian ignition date, (b) mean NDVI, (c) general topography (hilly or flat) and (d) mean FWI. Error bars represent one T_s standard deviation.

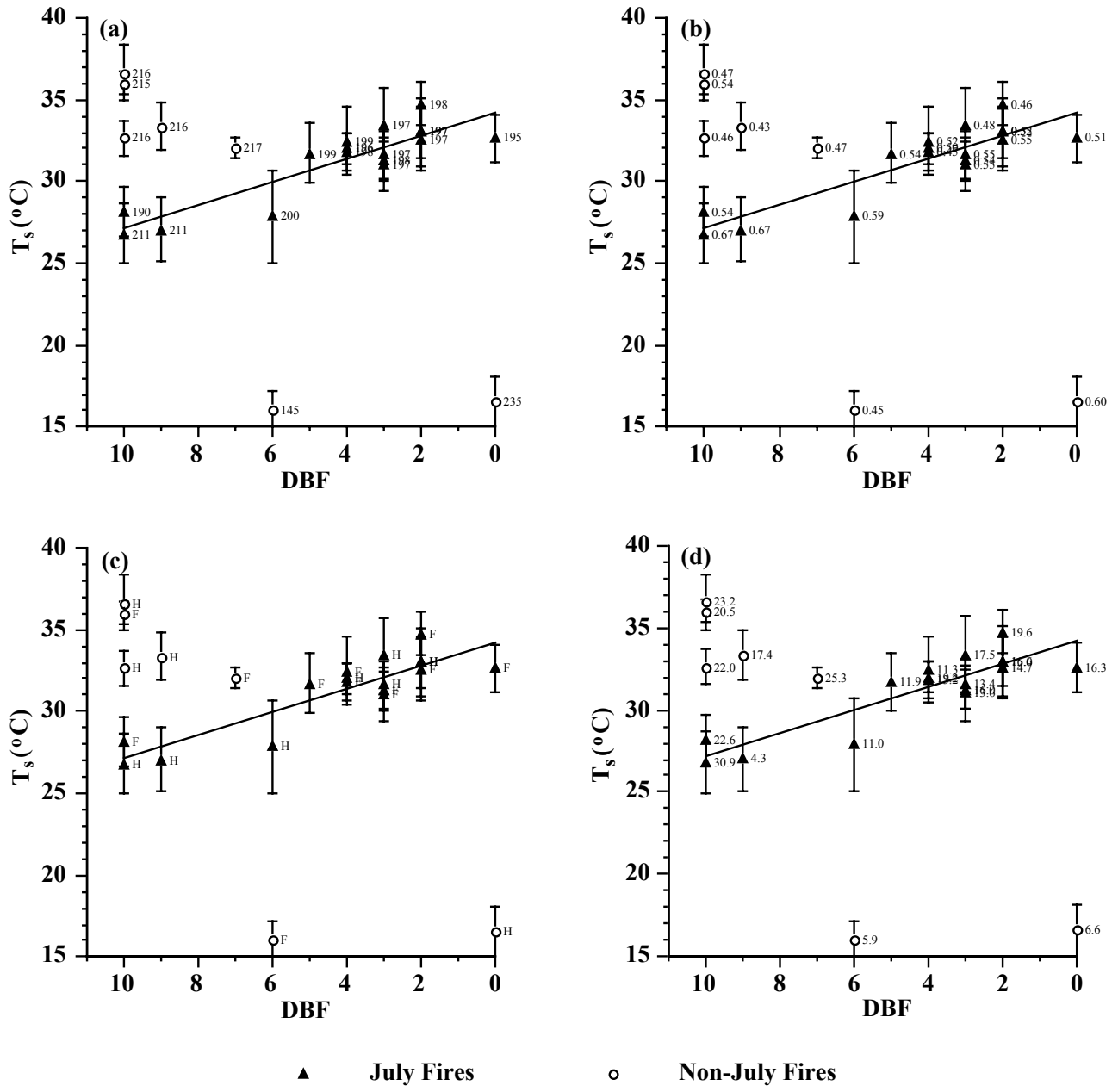


Figure 2 Scatter plots of mean T_s within unburned areas versus days before fire ignition, for fires starting and not starting in July, labeled with (a) Julian ignition date, (b) mean NDVI, (c) general topography (hilly or flat) and (d) mean FWI. Error bars represent one T_s standard deviation.

Mean T_s values of all fires combined exhibited no trend with an approaching fire ignition date (DBF). As already shown with mean values (Table 3), there was no significant difference between burned and unburned areas. What seemed to play a bigger role in the T_s - DBF relationship was the month when fires started. When non-July fires, i.e., not starting between Julian dates 182 and 212, were excluded from the analysis, T_s tended to increase with DBF on both burned (Figure 1) and unburned (Figure 2) areas. Among all the non-July fires, there were first fires starting at the beginning of August which showed high T_s nine and ten days before fire ignition. Two fires labeled “216” had no additional data during the 11 day period for the burned areas. One of these fires (fire “fs092”) showed decreasing mean T_s over the unburned area (Table 3 and Figure 2). The third fire, labeled “215”, showed a slight increasing in mean T_s , but there were no images available after 9 days before fire ignition. Another group of outliers were a fire starting in May (labeled “145”) and a fire starting late August (labeled “235”). In each case, mean T_s values were quite low on both burned and unburned images (Figures 1 and Figure 2). They may be related to cool temperature conditions as they occurred early or late in the fire season. Bourgeau-

Chavez et al. (1999) already found that excluding spring fires from FWI regression analysis greatly aided its significance. The first outliers were not related to a significantly different cover type, since mean NDVI values were similar to the July-starting fires (Figure 1b and Figure 2b). However, the May fire had a rather low NDVI value, since it was related to the beginning of the growing season and thus the greenness of the vegetation (understory and overstory) was not as full as in July, as observed by Goward et al. (1985), Kasischke and French (1997), and Leblon et al. (2001). These outliers were not related to changes in elevation because they occurred on both hilly and flat terrain similar to the July-starting fires (Figure 1c and Figure 2c). A fourth factor which could explain both trends and outliers was FWI which is a measure of drought levels (Figure 1d and Figure 2d). This factor cannot explain the first group of outliers corresponding to fires starting at the beginning of August, but the FWI was very low for both the spring fire and the late August fire. The relationship between T_s and FWI was investigated (Figure 3) because FWI, as a drought indicator, appeared to have a significant effect on T_s evolution.

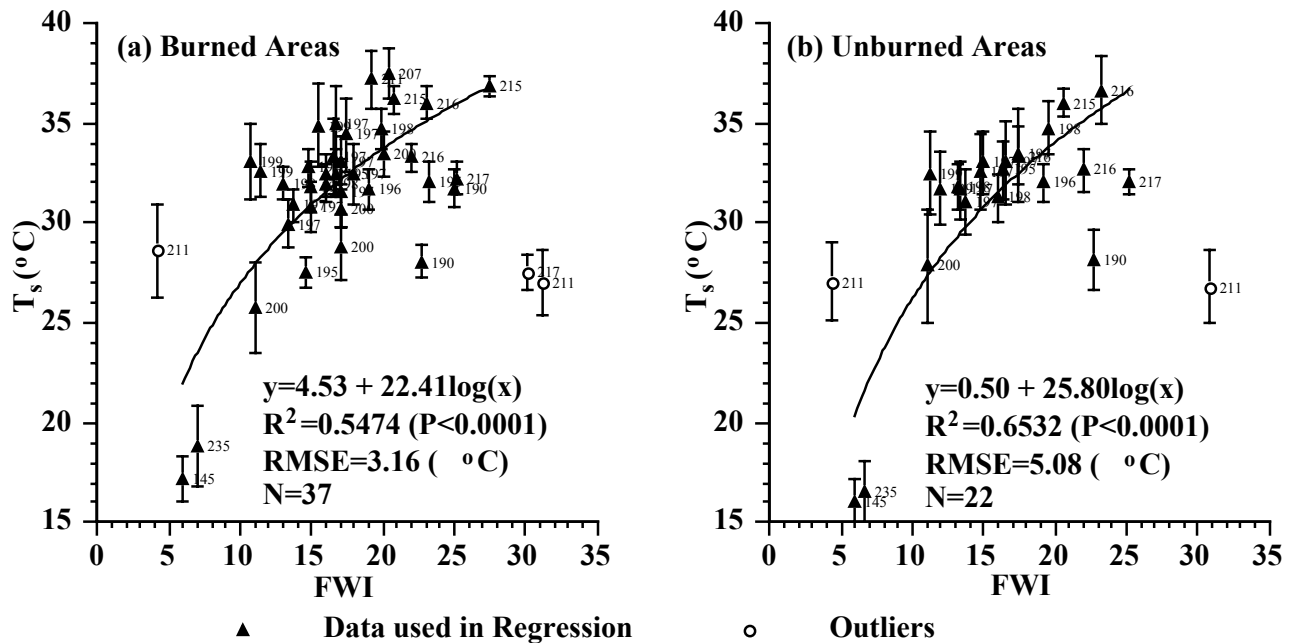


Figure 3 Scatter plots of mean T_s against FWI, for fires starting and not starting in July (labeled with Julian ignition date) within (a) burned areas and (b) unburned area. Error bars represent one T_s standard deviation.

A positive logarithmic trend was observed between the plots of T_s versus FWI. This indicates saturation in T_s once FWI reaches a certain level. Such a relationship could be indirect because both parameters were related to air temperature. Further research is needed in this regard. Among the set of outliers observed for both burned and unburned areas, there were those which first, exhibited moderate T_s and extreme FWI values (labeled “211” and “217”) and second, exhibited moderate T_s and low FWI values (labeled “211”). These values were likely related to environmental conditions at a particular weather station which need to be investigated further.

3.3. Use of NOAA-AVHRR images as fire danger mapping tool

To verify if NOAA-AVHRR thermal infrared images could be used to locate fire starts, images acquired before fire starts were examined. Such an analysis was only possible for some fires because of few clear images. One of the clearest sets of images was for fire “vq033”, which started on July 16. Within the burned and unburned zone of this fire, a very clear image was available on July 13, with 91% of the burned area clear and 62% of the unburned area clear. The FWI map showed high to very-high fire danger conditions (Figure 3a). The highest T_s values within the fire zone were located within and to the southwest of the burned area (Figure 3b). NDVI values within burned and unburned areas were fairly high (between 0.4-0.6) (Figure 2c). Such an example showed NDVI images were less useful for fire danger mapping than T_s , as T_s better represents droughtiness as indicated by FWI. However, both T_s and NDVI images show greater mapping details than FWI maps, confirming the usefulness of remote sensing as a mapping tool. FWI maps displayed large bands of FWI values and no weather station was located within the fire zone, whereas NOAA-AVHRR images display pixels of 1 km^2 .

However, the analysis of every image related to the fire was not enough to fully describe the fire behavior. This fire burned over 3 months (July 16 – October 5) and the ignition point was unknown. In addition, an important fire behavior parameter which should be considered in such an analysis is the wind. This cannot be derived from NOAA-AVHRR images. Wind directions and speeds can be mapped from images acquired over water bodies by the wind scatterometer on board of ERS-2. Thereby, a fire danger decision support system based on NOAA-AVHRR images should also have wind and topographic layers in order to predict fire behavior. In such a system, thermal infrared images can be used as a droughtness indicator.

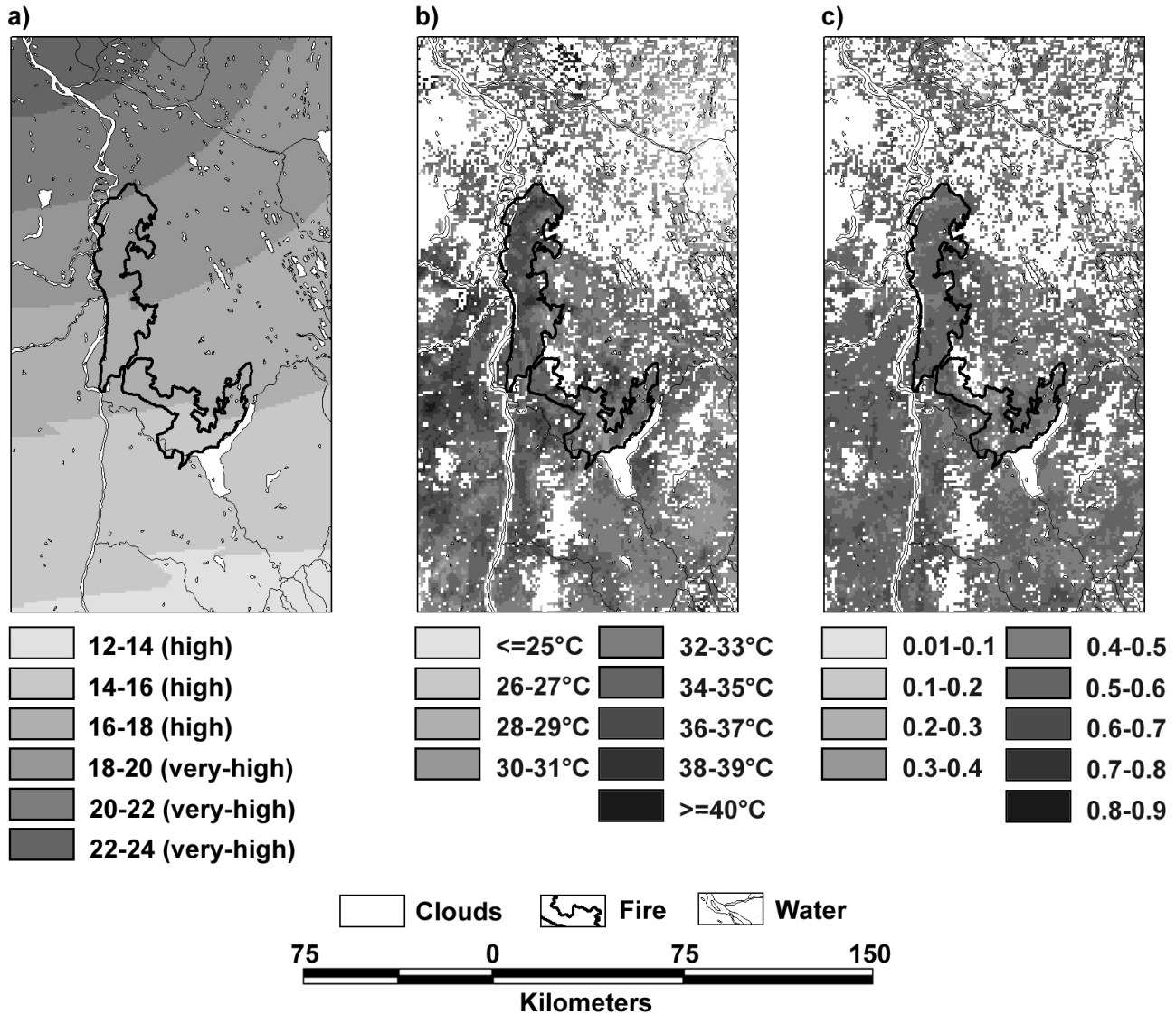


Figure 4 Map of (a) FWI, (b) T_s , (c) NDVI in the fire zone of fire vq033 on July 13 (3 days before fire ignition)

4. Conclusion

Presently in Canada fire danger is mapped by the CFFDRS system. This system is limited to produce estimates of fire danger for large geographic regions and does not consider environmental conditions at finer spatial scales. Thus, satellite remote sensing is a promising alternative. In this study the potential use of NOAA-AVHRR thermal infrared images, as indicators of fire danger, were examined. Attempts were made to map pre-fire T_s and NDVI conditions in the zones of 24 large forest fires occurring during the 1994 fire season in the Northwest Territories, Canada.

From fire zone images, acquired during the 11 day period prior to and on the day of fire ignition, a positive trend in mean T_s was observed as the day of fire ignition approached. A positive logarithmic trend was observed between mean T_s and mean FWI within burned and unburned areas. No significant difference was found between mean T_s values observed within burned and unburned areas. It was concluded that T_s can be used as a surrogate of FWI, but other factors such as wind should be considered to fully describe fire behavior. Another limitation was the low availability of clear NOAA 11-AVHRR images. In order to increase the availability of clear images during cloudy days, radar images could be incorporated as they can be used under any weather conditions. Leblon et al. (2001) has found good relationships between ERS-1 SAR radar backscatter and FWI codes. Further research is needed to develop methods to incorporate both NOAA-AVHRR and radar images in mapping fire danger.

5. Acknowledgements

This study was funded by NSERC and CIFFC. Images were obtained from J. Cihlar, Application Division of the CCRS.

6. References

- Bourgeau-Chevez LL, Kasischke ES, Rutherford MD (1999) Evaluation of ERS SAR data for prediction of fire danger in a boreal region. *Int. J. Wildland Fire* 9(3): 183-194
- Burgan RE, Hartford RA (1993) Monitoring vegetation greenness with satellite data. United States Department of Agriculture, Forest Service, General Technical Report INT-297, Intermountain Research Station, Ogden, Utah, 13 pp
- Burgan RE, Hartford RA, Eidenshink JC (1996) Using NDVI to assess departure from average greenness and its relation to fire business. United States Department of Agriculture, Forest Service, General Technical Report INT-GTR-333, Intermountain Research Station, Ogden, Utah, 8 pp
- Burgan RE, Klaver RW, Klaver JM (1998) Fuel models and fire potential from satellite and surface observations. *Int. J. Wildland Fire* 8(3): 159-170
- Canadian Council of Forest Ministers (2001) [Internet] National Forestry Database Program. Available from: <<http://nfdp.ccfm.org>>
- Canadian Forest Service (1987) Canadian Forest Fire Danger Rating System - Users's Guide. Fire Danger Group of the Canadian Forest Service, Ottawa, Ontario, Three-ring binder (unnumbered publication)
- Chuvieco E, Deshayes M, Stach N, Cocero D, Riano D, (1999) Short-term fire risk: foliage moisture content estimation from satellite data. In: Chuvieco E (ed.) *Remote Sensing of Large Wildfires in the European Mediterranean Basin*. Springer-Verlag, Berlin, pp 17-38
- Deblonde G, Cihlar J, (1993) A multiyear analysis of the relationship between surface environmental variables and NDVI over the Canadian landmass. *Remote Sens. Rev.* 7: 151-177
- Desbois N (1994) Suivi en temps réel de l'état hydrique des végétaux, par imagerie satellitaire NOAA-AVHRR. Application à la prévision du risque d'incendie en région méditerranéenne. Mémoire de D.A.A., INA Paris-Grignon et Laboratoire commun de télédétection CEMAGREF-ENGREF, 52 + annexes
- Debois N, Vidal A (1995) La télédétection dans la prévision des incendies de forêt. *Ingénieries-EAT* 1: 21-29
- Dominguez L, Lee BS, Chuvieco E, Cihlar J (1994) Fire danger estimation using AVHRR images in the Prairie provinces of Canada. In: *Proceedings of the 2nd Int. Conference on Forest Fire Research, Coimbra, Portugal* 2(17): 679-690
- Duchemin B, Guyon D, Lagouarde JP (1999) Potential and limits of NOAA- AVHRR temporal composite data for phenology and water stress monitoring of temperate forest ecosystems. *Int. J. Remote. Sens.* 20(5): 895-917
- Flannigan MD, Wotton BM (1989) A study of interpolation methods for forest fire danger rating in Canada. *Can. J. For. Res.* 19: 1059-1066
- Gallant L, (1998) Suivi, par imagerie NOAA-AVHRR, de l'état hydrique de peuplements de conifères du bassin du fleuve Mackenzie (Territoires du Nord-Ouest) dans une perspective de prévision du danger d'incendie de forêt. Master thesis, Department of Geography and Remote Sensing, University of Sherbrooke (Quebec), 104 pp
- Geogratis Canada (2001) [Internet] Digital elevation map of Canada. Available from: <http://geogratis.cgdi.gc.ca/download/gtopo30/canada_dem.zip>
- Goita K, Royer A, Bussièrès N (1997) Characterization of land surface thermal structure from NOAA-AVHRR data over a northern ecosystem. *Remote Sens. Environ.* 60: 282-298
- Goward SN, Cruickshanks GD, Hope AS (1985) Observed relation between thermal emission and reflected spectral radiance of a complex vegetated landscape. *Remote Sens. Environ.* 18: 137-146
- Hardy CC, Burgan RE (1999) Evaluation of NDVI for monitoring live moisture in three vegetation types of the Western U.S. *Photogram. Eng. Remote Sens.* 65: 603-610
- Huemrich KF, Black TA, Jarvis PG, McCaughey JH, Hall, FG (1999) High temporal resolution NDVI phenology from micrometeorological radiation sensors. *J. Geophysical Res.* 104: 27935-27944

- Illera P, Fernandez A, Delgado JA (1996) Temporal evolution of the NDVI as an indicator of forest fire danger. *Int. J. Remote. Sens.* 17(6): 1093-1105
- Kasischke E, French NH (1997) Constraints on using AVHRR composite index imagery to study patterns of vegetation cover in boreal forests. *Int. J. Remote Sens.* 18: 2403-2426
- Leblon B (2001) Forest wildfire hazard monitoring using remote sensing: a review. *Remote Sensing Reviews* 20(11): 1-44
- Leblon B, Alexander M, Chen J, White S (2001) Monitoring fire danger of northern boreal forests with NOAA-AVHRR NDVI images. *Int. J. Remote Sensing* 22: 2839-2846
- Nemani RR, Running SW (1989) Estimation of regional surface resistance to evapotranspiration from NDVI and thermal-IR AVHRR data. *J. Applied Meteorology* 28(4): 276-284
- Nemani RR, Pierce L, Running S, Goward S (1993) Developing satellite-derived estimates of surface moisture status. *J. Applied Meteorology* 32: 548-557
- Paltridge GW, Barber J (1988) Monitoring grassland dryness and fire potential in Australia with NOAA-AVHRR data. *Remote Sens. Environ.* 25: 381-394
- Pierce LL, Running SW, Riggs GA (1990) Remote detection of canopy water stress in coniferous forests using the NS001 Thematic Mapper Simulator and the Thermal Infrared Multispectral Scanner. *Photogram. Eng. Remote Sens.* 56(5): 579-586
- Prince SD, Goetz SD, Dubayah RO, Czajkowski KP, Thawley M (1998) Inference of surface and air temperature, atmospheric precipitable water and vapor pressure deficit using Advanced Very High Resolution Radiometer satellite observations: compared with field observation. *J. Hydrology* 212-213: 230-249
- Prosper-Laget V, Wigneron JP, Guinot JP, Seguin B (1995) Utilisation du satellite NOAA pour la détection des risques d'incendies de forêts. *La Météorologie* 8(10): 28-38
- Robertson BA, Erickson A, Friedel J, Guindon B, Fisher T, Brown R, Teillet P, D'Iorio M, Cihlar J, and Sancz A (1992) GEOCOMP, a NOAA-AVHRR geocoding and composition system. In: *Proceedings of the ISPRS Conference, Commission II, Washington, D.C.* pp 223-228
- Rothman DS, Herbert D (1997) The socio-economic implications of climate change in the forest sector of the Mackenzie basin. In: Cohen SJ (ed.) *Mackenzie Basin impact study (MBIS), Final Report*, pp 225-241
- Rowe JS (1972) *Forest regions of Canada*. Canadian forestry service publication no. 1300. Ottawa, Ontario 172 pp
- Schmidt H, Gitelson A (2000) Temporal and spatial vegetation cover changes in Israeli transition zone: AVHRR-based assessment of rainfall impact. *Int. J. Remote Sens.* 21: 997-1010
- Stocks BJ, Lawson BD, Alexander ME, Van Wagner CE, McAlpine RS, Lynham TJ, Dube DE (1989) The Canadian Forest Fire Danger Rating System: an overview. *The Forestry Chronicle* 65: 450-457
- Strickland G, Leblon B, Gallant L, Alexander ME (2001) Fire danger monitoring using NOAA-AVHRR images. Accepted in *Can. J. Remote Sens.*
- Van Wagner CE (1990) Six decades of forest fires science in Canada. *The Forestry Chronicle* 66: 133-137
- Vidal A, Pinglo F, Durand H, Devaux-Ros C, Maillet A (1994) Evaluation of a temporal fire risk index in Mediterranean forests from NOAA thermal IR. *Remote Sens. Environ.* 49: 296-303